ELSEVIER

Journal of Photochemistry and Photobiology A: Chemistry 156 (2003) 45–54

Journal of Photochemistry and Photobiology A:Chemistry

www.elsevier.com/locate/jphotochem

Synthesis and photophysical properties of *N*,*N*′-bis(4-cyanophenyl)-3,4,9,10-perylenebis(dicarboximide) and *N*,*N*′-bis(4-cyanophenyl)-1,4,5,8-naphthalenediimide

Duygu Uzun [a], Mustafa E. Ozser [b], Kivanc Yuney [a], Huriye Icil [a,*], Martin Demuth [b]

[a] *Department of Chemistry, Faculty of Arts and Science, Eastern Mediterranean University, Famagusta, N. Cyprus, Mersin 10, Turkey*
[b] *Max-Planck-Institut für Strahlenchemie, D-45413 Mülheim an der Ruhr, Germany*

Received 10 April 2002; received in revised form 5 November 2002; accepted 3 December 2002

Abstract

N,*N*′-Bis(4-cyanophenyl)-1,4,5,8-naphthalenediimide (CN-NDI) and *N*,*N*′-bis(4-cyanophenyl)-3,4,9,10-perylenebis(dicarboximide) (CN-PDI) have been synthesized under special conditions in high yield. The compounds are characterized by UV-Vis, IR, NMR, MS, DSC, TGA and CV measurements. The fluorescence lifetimes, quantum yields and singlet-state energies are presented. CN groups at the phenyl moieties improve the thermal stability of the compounds. The LUMO energy values, −3.91 eV (CN-NDI in solution) and −3.96 eV (CN-NDI and CN-PDI at solid state), are determined by cyclic voltammetry. Whereas CN-NDI shows two reversible (−0.89 and −1.34 V) reduction steps (vs. Fc) in solution, CN-NDI and CN-PDI exhibit only one reversible wave at −0.48 V vs. Ag/AgCl at solid state, assigned to the one-electron reduction. Formation of aggregates shifts the UV absorption spectrum of CN-PDI to shorter wavelengths and its lifetime is measured as 4.6 ns at 580 nm. CN-PDI may be a promising dye for organic solar cells.

Keywords: *N*,*N*′-Bis(4-cyanophenyl)-3,4,9,10-perylenebis(dicarboximide); *N*,*N*′-Bis(4-cyanophenyl)-1,4,5,8-naphthalenediimide; Aggregation; Electron transfer reactions; Organic solar cells

1. Introduction

Perylenediimides, due to their outstanding chemical, thermal and photochemical stability, are highly promising materials for applications in organic solar cells, photovoltaic devices and for dye lasers [1–4]. On the other hand, 1,4,5,8-naphthalenediimides have been used for the preparation of electronical conducting materials, Langmuir–Blodgett films, π-stacked materials absorbing in the near-IR region and models for the photosynthetic reaction center [5,6]. The main reason of the increasing interest for these dyes originates from their electron acceptor properties and the photochemical stability [7].

Organic materials for the production of organic solar cells are attractive with regard to the price and the easy handling. Their application needs suitable physical, chemical, electrophysical, photochemical and mechanical properties which are met with a number of perylenediimides giving the impetus for growing interest in this field [8,9].

Cyanoaromatics are generally known for their excellent electron acceptor properties. In the present paper we focus attention on the synthesis of *N*,*N*′-bis(4-cyanophenyl)-1,4,5,8-naphthalenediimide (CN-NDI) and *N*,*N*′-bis(4-cyanophenyl)-3,4,9,10-perylenebis(dicarboximide) (CN-PDI) as shown in Scheme 1. However, the so far known procedure for the preparation of perylenediimides [10,11] did not work for the CN-substituted derivatives CN-NDI and CN-PDI described in this paper. In this respect, the procedure has been improved. The optical, photochemical, thermal and electrochemical properties of these successfully synthesized compounds have then been determined. Furthermore, the applicability of these dyes as electron acceptors is discussed.

2. Experimental details

2.1. Materials

1,4,5,8-Naphthalene tetracarboxylic dianhydride, perylene-3,4,9,10-tetracarboxylic dianhydride, 4-aminobenzonitrile, isoquinoline, *m*-cresol and zinc acetate were obtained from Aldrich. Tetrabutylammonium hexafluorophosphate

* Corresponding author. Tel.: +90-392-6301085.
E-mail address: huriye.icil@emu.edu.tr (H. Icil).

1010-6030/03/$ – see front matter © 2003 Elsevier Science B.V. All rights reserved.
doi:10.1016/S1010-6030(02)00436-7

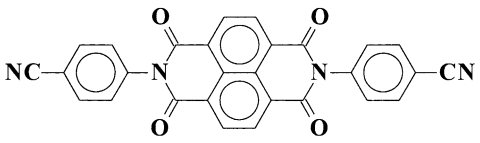

CN-NDI

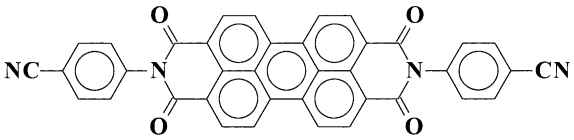

CN-PDI

Scheme 1.

(TBAPF6) and ferrocene were purchased from Fluka. *N*,*N*′-Bis-phenyl-1,4,5,8-naphthalenediimide (Phenyl-NDI) and *N*,*N*′-bis-phenyl-3,4,9,10-perylenebis(dicarboximide) (Phenyl-PDI) were synthesized for thermal stability comparison according to our general procedure [11]. All organic solvents employed were of spectroscopic grade.

2.2. Spectroscopic measurements

UV absorption spectra of solutions were measured with a Varian-Cary 100 spectrophotometer, spectra of solid state samples with a Perkin Elmer UV/VIS/NIR Lambda 19 instrument and infrared spectra with a Bruker IFS 66 (FT-IR) spectrophotometer. Mass spectra were measured with a Finnigan-MAT 311A instrument. Emission spectra were obtained with a Spex fluorolog. Elemental analyses were gained with a Carlo Erba-1106 C, H, N analyzer. ^{1}H and ^{13}C NMR spectra were measured with a Bruker AC 270. TGA thermograms were obtained from a Tg-Ms: Simultane TG–DTA/DSC apparatus STA 449 Jupiter from Netzsch, equipped with Balzers Quadstar 422 V. In measurements 1.820 mg CN-NDI and 3.99 mg CN-PDI were heated at 5 K/min in oxygen. Thermal analyses were obtained from a DSC 820 Mettler Toledo instrument. The 4.077 mg from CN-NDI and 7.149 mg from CN-PDI were heated at 5 K/min in nitrogen. Cyclic voltammetry (CV) in solvents was performed using a three-electrode cell with a polished 2 mm glassy carbon as working and Pt as counter electrode; solutions were 10^{-3} M in electroactive material and 0.10 M in supporting electrolyte TBAPF6. Data were recorded on an EG&G PAR 273A computer-controlled potentiostat. Ferrocene was used as internal reference. A scan rate of 100 mV s^{-1} for CN-NDI was employed for CV (solvent: chloroform). CV in solid state was performed using an AUTOLAB system (Eco-Chemie, Utrecht, The Netherlands). The reference electrode was an Ag/AgCl electrode (saturated NaCl) with a potential of 0.200 V vs. SHE at 25 °C. A platinum wire served as an auxiliary electrode. A graphite rod (diameter: 0.5 cm) was used as working electrode. Both compounds were immobilized at the surface of the paraffin impregnated graphite electrodes (PIGEs) with a diameter of 5 mm [12]. The solid compound was attached to the surface of PIGE by scratching. The supporting electrolyte was 1 M $NaClO_4$. A scan rate of 100 mV s^{-1} was employed for solid state voltammetry. Fluorescence lifetime measurements were performed by time correlated single photon counting technique (FLS920, Edinburgh Instruments).

2.3. Synthesis

In general, naphthalene and perylenediimides are described to be readily synthesized via condensation of the appropriate amine with the commercially available 1,4,5,8-naphthalene tetracarboxylic dianhydride and perylene-3,4,9,10-tetracarboxylic dianhydride using a *m*-cresol/isoquinoline mixture as the solvent [11]. However, the synthesis of CN-NDI and CN-PDI could not be prepared according to this general procedure. Existence of the electron accepting cyano group in the amine presumably prevents the imide formation. Syntheses of CN-NDI and CN-PDI were finally accomplished in our hands under nitrogen atmosphere in rigorously dried solvents and $Zn(OAc)_2{\cdot}2H_2O$. CN-NDI and CN-PDI were obtained with very high yield and could be purified easily. Their structures were identified by elemental analysis, IR, MS and NMR spectroscopy.

2.3.1. CN-NDI

The 1.0 g (3.7 mmol) 1,4,5,8-naphthalene tetracarboxylic dianhydride, 0.90 g (7.5 mmol) 4-aminobenzonitrile and 0.80 g (3.7 mmol) $Zn(OAc)_2{\cdot}2H_2O$ were heated in a carefully dried solvent mixture (60 ml *m*-cresol and 10 ml isoquinoline) under nitrogen atmosphere at 80 °C for 8 h, 100 °C for 8 h, 120 °C for 5 h, 140 °C for 8 h, 160 °C for 8 h, 180 °C for 4 h and finally at 200 °C for 6 h. The solution was allowed to cool and was poured into 300 ml acetone. The precipitate was filtered off and dried at 100 °C under vacuum. The crude product was treated with acetone in a Soxhlet apparatus for 1 day in order to get rid of the unreacted amine, zinc acetate and high boiling solvents. The 1.6 g (92%) CN-NDI was obtained as a yellow solid. $R_f = 0.1$ ($CHCl_3$); IR, ν (KBr pellets, cm^{-1}): 3097, 3066, 3051, 2234, 1713, 1677, 1576, 1507, 1448, 1439, 1352, 1249, 1202, 1140, 1023, 982, 898, 860, 847, 771, 752, 705, 580, 560, 409. UV-Vis, λ_{max} (DMF, nm) (ε, l mol^{-1} cm^{-1}): 380 (43 900), 360 (38 900), 344 (25 000). Fluorescence, λ_{max} (DMF, nm): 403. $Q_f = 0.003$. MS, $m/z = 468$ (M^+): 424, 379, 350, 322, 278, 252, 234, 152, 124, 74, 51. ^{1}H NMR, δ_H (ppm) (250 MHz, $CDCl_3 + C_2F_3O_2D$, 5:3): 8.99 (s, 4Ar–H, H–C(2), H–C(3), H–C(6), H–C(7)), 7.98 (d, J = 8.45 Hz, 4Ar–H, H–C(15), H–C(17), H–C(21), H–C(23)), 7.59 (d, J = 8.45, 4Ar–H, H–C(14), H–C(18), H–C(20), H–C(24)) (Fig. 1 and Scheme 2). ^{13}C NMR, δ_C (ppm) (250 MHz, $CDCl_3 + C_2F_3O_2D$, 5:3): 163.79 (4C=O, C(9), C(10), C(11), C(12)), 138.40 (2C–N, C(13), C(19)), 134.06 (4Ar–CH, C(15), C(17), C(21), C(23)), 132.70 (4Ar–CH, C(14), C(18), C(20), C(24)), 129.80 (4Ar–CH, C(2), C(3),

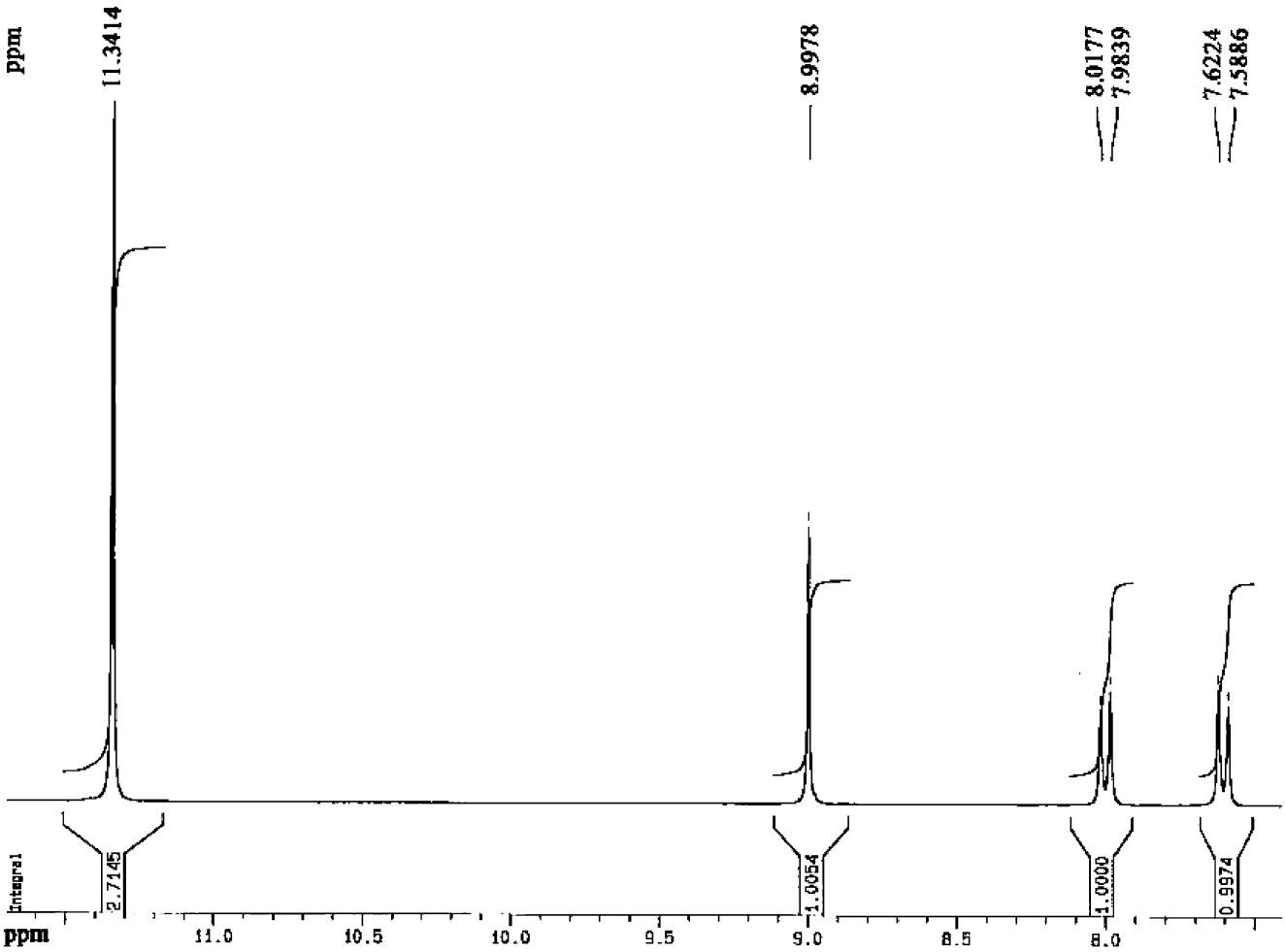

Fig. 1. ^{1}H NMR spectrum of CN-NDI in $CDCl_3 + C_2F_3O_2D$ (5:3).

C(6), C(7)), 127.19 (2(C), C(25), C(26)), 126.61 (4(C), C(1), C(4), C(5), C(8)), 112.50 (2(C), C(27), C(28)) (Fig. 2 and Scheme 2). Anal. Calcd. for $C_{28}H_{12}N_4O_4$: C, 71.79; H, 2.58; N, 11.96. Found: C, 70.89; H, 2.16; N, 11.38.

2.3.2. CN-PDI

The 1.0 g (2.6 mmol) 3,4,9,10-perylene tetracarboxylic dianhydride, 0.60 g (5.1 mmol) 4-aminobenzonitrile and 0.60 g (2.6 mmol) $Zn(OAc)_2{\cdot}2H_2O$ were heated in a carefully dried solvent mixture (60 ml *m*-cresol and 10 ml isoquinoline) under nitrogen atmosphere at 100 °C for 12 h, 140 °C for 5 h, 160 °C for 13 h, 180 °C for 16 h, 200 °C for 44 h and finally at 220 °C for 5 h. The solution was allowed to cool and then was poured into 300 ml acetone. The precipitate was filtered off and dried at 100 °C under vacuum. The crude product was washed several times with 2% aqueous NaOH until the characteristic green fluorescing color of perylene dianhydride disappeared prior to treatment with chloroform in a Soxhlet apparatus for 1 day in order to get rid of the unreacted amine, the catalyst zinc acetate and high boiling solvents. The 1.1 g (72%) CN-PDI was obtained as a dark red solid. R_f = 0.09 ($CHCl_3$); IR, ν (KBr pellets, cm^{-1}): 3520, 3110, 2234, 1698, 1670, 1594, 1574, 1508, 1403, 1356, 1344, 1253, 1175, 1135, 856, 845, 798, 744, 559, 466. UV-Vis, λ_{max} (DMF, nm): 462, 490, 526, 579. Fluorescence, λ_{max} (DMF, nm): 537, 579, 629. MS, m/z = 592 (M^+): 548, 492, 446, 376, 282, 223, 168, 108, 90, 79. ^{1}H NMR, δ_H (ppm) (250 MHz, $CDCl_3 + C_2F_3O_2D$, 5:3): 8.91 (s, 8Ar–H, H–C(1), H–C(2), H–C(5), H–C(6), H–C(7), H–C(8), H–C(11), H–C(12)), 7.96 (d, 4Ar–H, H–C(19), H–C(21), H–C(25), H–C(27)), 7.61 (d, 4Ar–H, H–C(18), H–C(22), H–C(24), H–C(28)) (Fig. 3 and Scheme 2). ^{13}C NMR, δ_C (ppm) (250 MHz, $CDCl_3 + C_2F_3O_2D$, 5:3): 164.94 (4C=O, C(13), C(14), C(15), C(16)), 136.24 (2C–N, C(17), C(23)), 134.05 (4Ar–C, C(2), C(5), C(8), C(11)), 133.51 (4Ar–C, C(1), C(6), C(7), C(12)), 129.91 (4Ar–C,

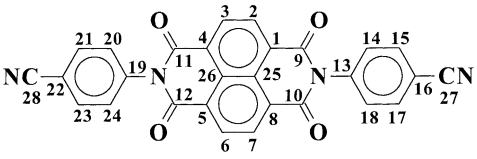

Scheme 2.

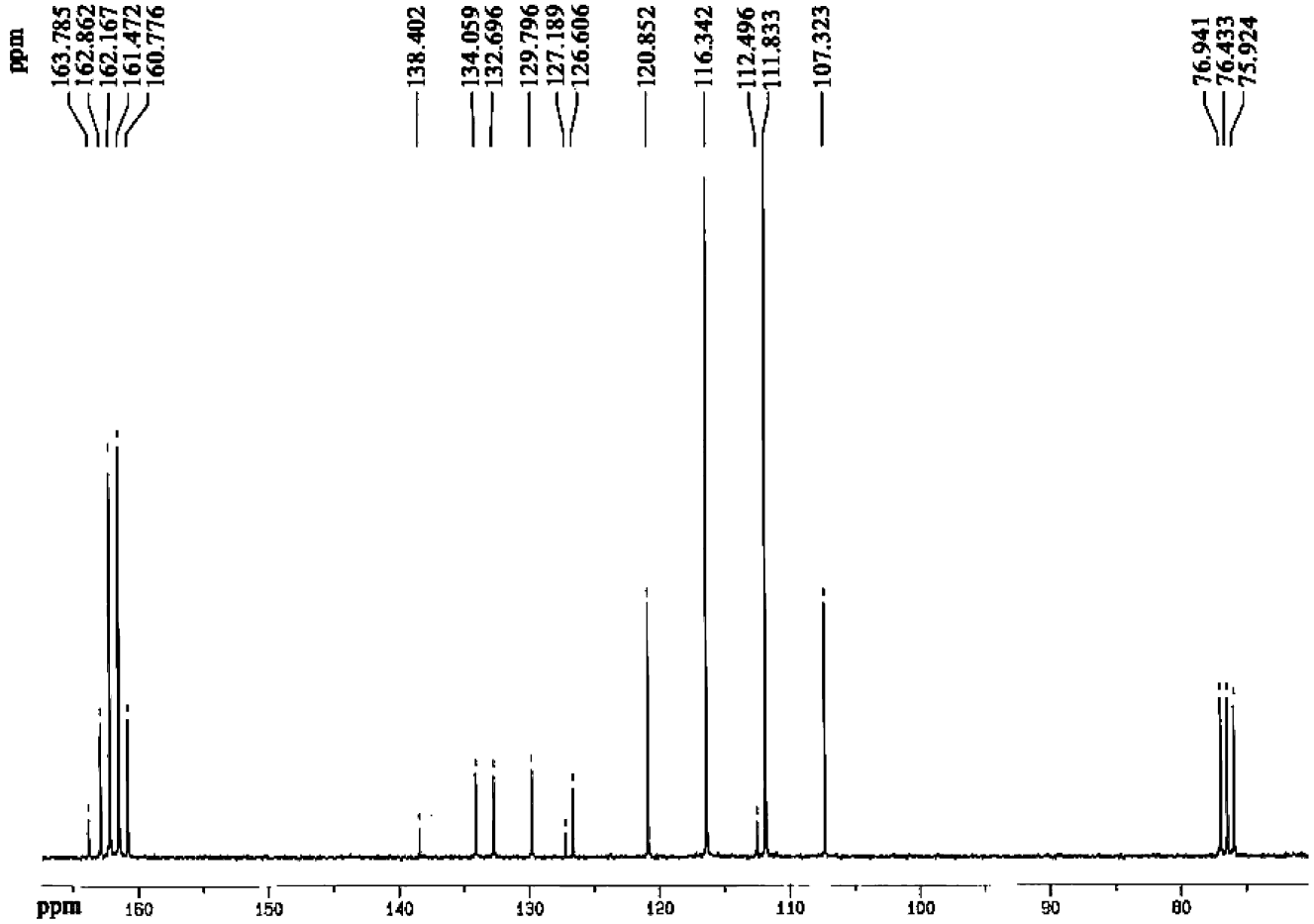

Fig. 2. ^{13}C NMR spectrum of CN-NDI in $CDCl_3 + C_2F_3O_2D$ (5:3).

C(19), C(21), C(25), C(27)), 124.52 (4Ar–C, C(18), C(22), C(24), C(28)), 122.12 (4Ar–C, C(3), C(4), C(9), C(10)), 76.79 (2Ar–C, C(20), C(26)) (Fig. 4 and Scheme 2). Anal. Calcd. for $C_{38}H_{16}N_4O_4$: C, 77.02; H, 2.72; N, 9.45. Found: C, 76.57; H, 2.55; N, 8.64.

3. Results and discussion

3.1. Spectral characteristics of CN-NDI and CN-PDI

The solubility of CN-NDI and CN-PDI in different solvents is given in Table 1. Whereas the solubility of both compounds is poor in non-polar solvents it increases in polar media.

Table 1
Solubility of CN-NDI and CN-PDI

	Solubility[a]/color			
	$CHCl_3$	Acetone	DMF	DMSO
CN-NDI	(−+), yellow	(−+), yellow	(++), yellow	(++), yellow
CN-PDI	(−+), red	(++), red	(++), red	(−+), red

[a] (++) soluble at room temperature; (−+) soluble on heating at 60 °C; the solubility increases upon heating.

The UV absorption spectrum of CN-NDI shows characteristically three bands at 344, 360 and 380 nm in DMF. The emission spectrum of the CN-NDI was taken at λ_{exc} = 360 nm with anthracene as standard. The fluorescence spectrum exhibits mirror symmetry for the 0–0 absorption and 0–0 emission bands, but not for the bands at 360 and 344 nm, indicating some structural changes of CN-NDI upon excitation. The spectrum of CN-NDI (Fig. 5a) shows no aggregation characteristics. In contrast, CN-PDI exhibits a broad visible-light absorption (400–700 nm) with the absorption maxima (Fig. 5b) at 462, 490 and 526 nm (DMF). The new absorption band observed at 579 nm, as compared to non-CN-substituted PDIs, is attributed to aggregation. The absorption characteristics of CN-PDI in DMF, i.e. shift of the maxima together with a strong increase of absorbance, are interpreted as aggregation phenomenon. The UV spectra of CN-NDI and CN-PDI in different solvents are shown in Fig. 6. The CN-NDI absorption maxima do not depend on the polarity of solvent. The maximum absorption wavelengths of CN-PDI are shifted to the red region in chloroform being a characteristic example for the

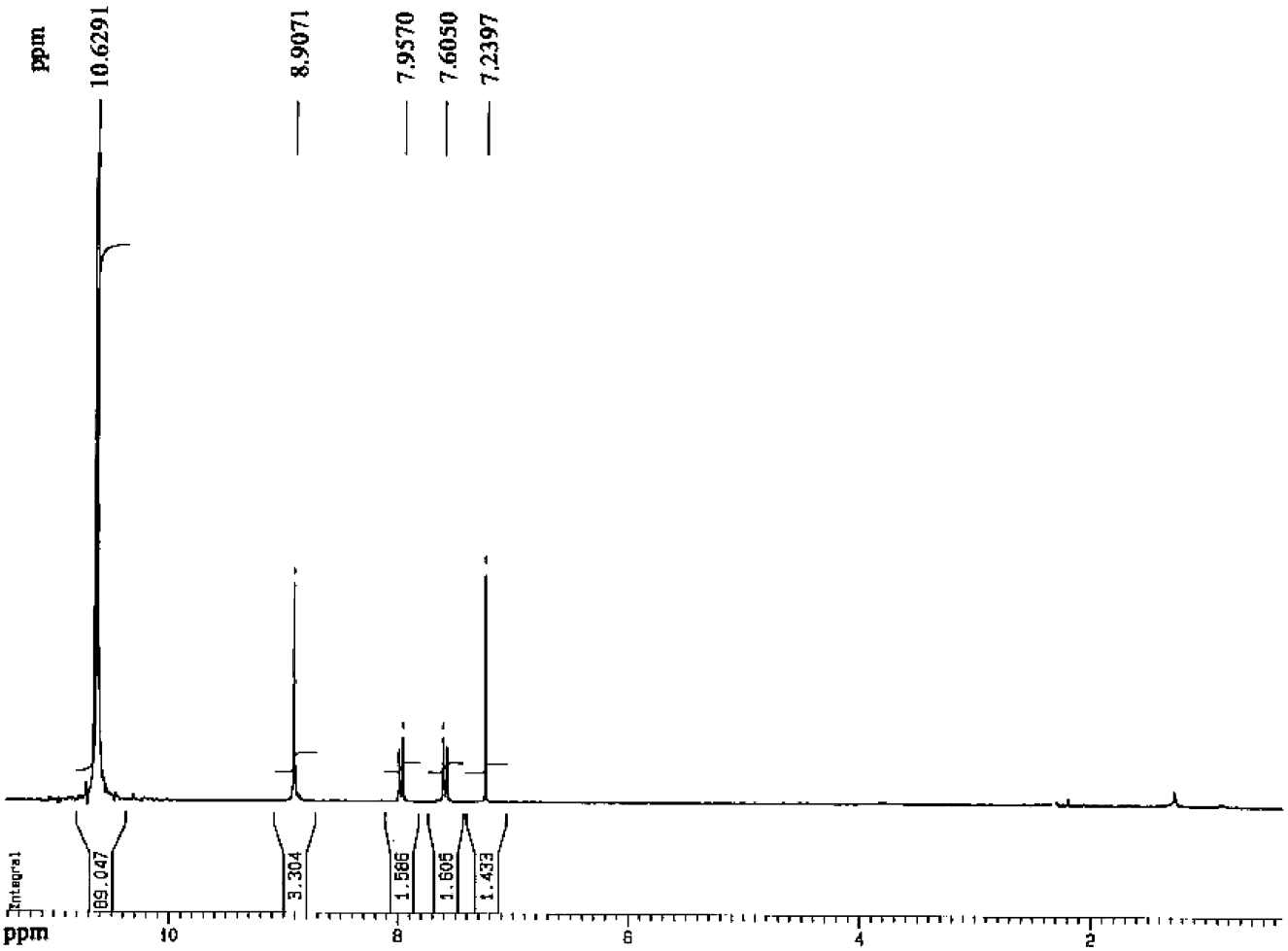

Fig. 3. ^{1}H NMR spectrum of CN-PDI in $CDCl_3 + C_2F_3O_2D$ (5:3).

spectroscopic behavior of this perylenediimide in non-polar solvents. Further, the new absorption band at 579 nm, being ascribed to aggregation, disappears upon filtration of the solution through a 0.2 μm SPR microfilter.

The emission spectrum of the CN-PDI was taken at $\lambda_{exc} = 485$ nm with perylene-3,4,9,10-tetracarboxylic acid–bis-*N*,*N*′-dodecyl diimide as standard. The fluorescence quantum yields of CN-NDI and CN-PDI are measured as 0.003 and 0.136, respectively. The low fluorescence quantum yield of CN-NDI is in good correlation with literature data [13] and shows a fast deactivation of the S_1 state, probably via intersystem crossing to a close-lying triplet state. On the other hand, the low fluorescence quantum yield of CN-PDI, which contrasts the data of non-CN-substituted PDIs, we attribute to the existence of molecular aggregation of CN-PDI under the given conditions. The overlap between the absorption and emission spectra of the compound would lead to re-absorption of the emitted photons by ground state CN-PDI offering, in our opinion, new application possibilities in the field of solar technology (Fig. 5b).

Peak positions of absorption (λ_{max} in nm, DMF), fluorescence quantum yields (Q_f, DMF), radiative lifetimes τ_0 (ns), fluorescence lifetimes τ_f (ns), fluorescence rate constants k_f ($\times 10^8\ s^{-1}$), and singlet energies E_s (kcal mol^{-1}) data of CN-NDI and CN-PDI in DMF, are given in Table 2. The fluorescence intensity of CN-NDI in methyl THF, even

Table 2
Peak positions of absorptions λ_{max} (nm) and extinction coefficients ε (l mol^{-1} cm^{-1}), fluorescence quantum yields Q_f, radiative lifetimes τ_0 (ns), fluorescence lifetimes τ_f (ns), fluorescence rate constants k_f ($\times 10^8\ s^{-1}$), and singlet energies E_s (kcal mol^{-1}) data of CN-NDI and CN-PDI in DMF

	CN-NDI	CN-PDI	
λ_{max} (ε)	344 (24955)	462	
	360 (38900)	490	
	380 (43898)	526	
		579	
Q_f	0.003	0.136	
λ_{exc} (λ_{em})	380	530 (580)	580 (650)
τ_0	7.6	–	–
τ_f[a]	0.023	(3.8)	(4.6)
k_f	1.3	–	–
E_s	75.3	54	49.3

[a] Experimental values are given in parentheses.

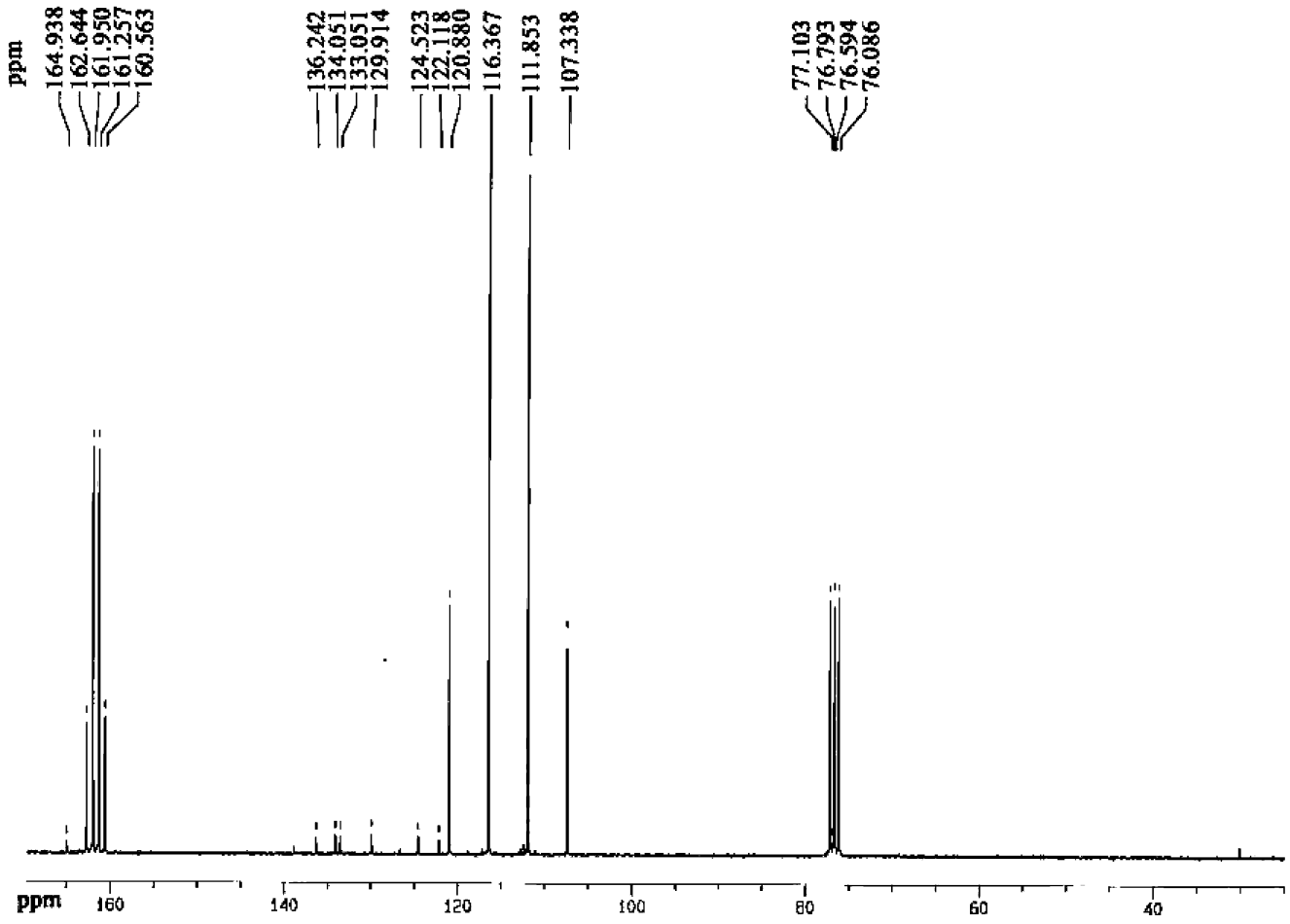

Fig. 4. ^{13}C NMR spectrum of CN-PDI in $CDCl_3 + C_2F_3O_2D$ (5:3).

after freeze–thaw cycles in liquid nitrogen, is the same. Fluorescence lifetimes of the compounds are measured in argon-saturated solutions. No phosphorescence could be detected from the CN-NDI solutions.

The theoretical radiative lifetimes τ_0 were calculated according to the formula: $\tau_0 = 3.5 \times 10^8/\nu^2_{max}\varepsilon_{max}\Delta\nu_{1/2}$, where ν_{max} stands for the wavenumber in cm^{-1}, ε_{max} for the molar extinction coefficient at the selected absorption wavelength and $\Delta\nu_{1/2}$ indicates the half-width of the selected absorption in units of cm^{-1} [14]. Fluorescence lifetimes are calculated from $\tau_f = \tau_0 Q_f$ and the rates of fluorescence from $k_f = 1/\tau_0$ (Table 2). The fluorescence lifetime of CN-NDI is calculated as 23 ps and supports the ultra fast intersystem crossing from the singlet excited state. The observed fluorescence lifetime of the compound was shorter than our available detection limit for emission (100 ps). These results are in reasonable correlation with the literature data [15,16]. The CN-PDI fluorescence lifetime is observed experimentally as 3.8 ns (λ_{exc} = 530 nm and λ_{em} = 580 nm, Fig. 7a). The emission at 650 nm (Fig. 7b), which is attributed to aggregation, exhibits a longer lifetime of 4.6 ns.

3.2. Aggregation of CN-PDI

A new band at 579 nm is observed even at 10^{-5} M concentration. Low fluorescence quantum yield is also attributed to molecular aggregation. In chloroform the solubility of the CN-PDI decreases comparing to DMF and DMSO and the tendency towards aggregation is very strong (Figs. 6b and 8). The spectral data of the unaggregated form is very similar to that of solutions (Fig. 8). Also a red shift is observed for all the bands in chloroform. Increasing dye concentration changes the intensity of the new band relative to the other bands. In polar solvents (DMF, DMSO) the aggregation band intensity of aggregates is lower than the others bands and increases as the concentration increases (Fig. 8). Meanwhile at higher concentration a blue shift is observed for the highest absorption band (Fig. 8). In chloroform the intensity of the aggregation band is more intense than the other absorptions and it notably disappears upon filtration of the solutions through a 0.2 μm SPR microfilter (Fig. 8). For CN-NDI the absorption maxima were the same in chloroform, DMF and DMSO. The solid state absorption spectrum of CN-NDI is given in Fig. 9. The absorption

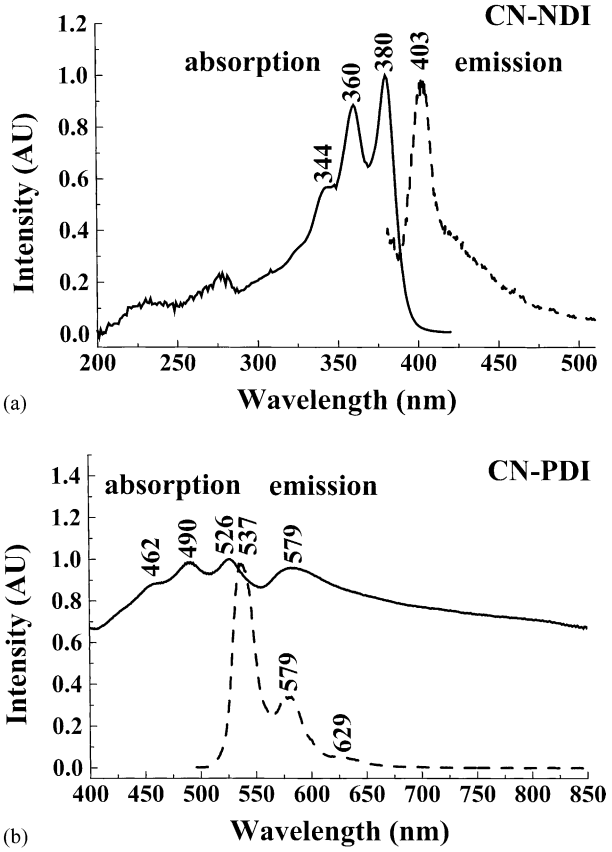

Fig. 5. Absorption and emission spectra of CN-NDI, $\lambda_{exc} = 360$ nm (a) and CN-PDI, $\lambda_{exc} = 485$ nm (b) in DMF.

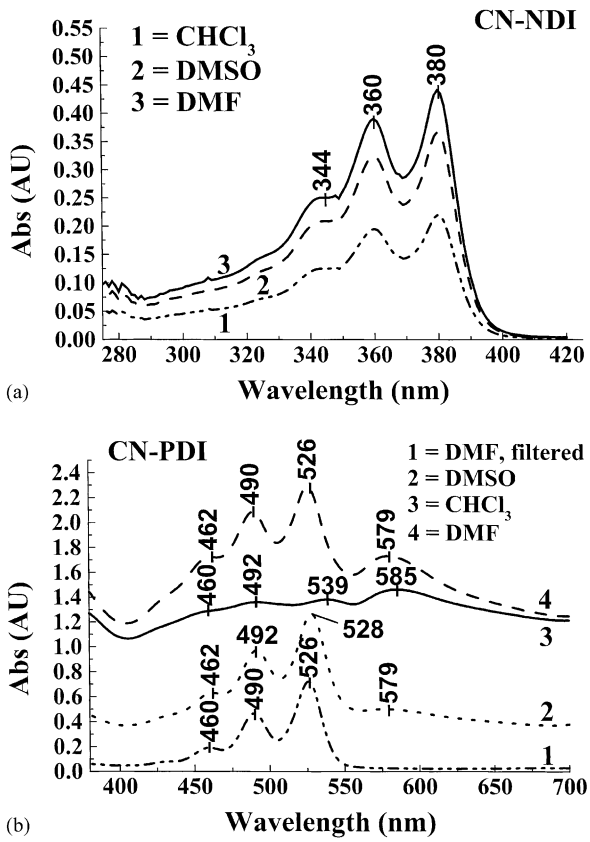

Fig. 6. Absorption spectra of CN-NDI (a) and CN-PDI (b) in $CHCl_3$, DMF and DMSO (10^{-5} M).

maxima are red shifted by about 15 nm while the fine structure remains essentially the same. This view supports the weak intermolecular interaction in the solid state.

The shapes of the absorption spectra of CN-PDI in solution and in the solid state show drastic differences in contrast to CN-NDI, in view of wavelength range (absorption up to 700 nm) and peak positions (Figs. 6a and 9). This spectral change is attributed to intermolecular π interaction in the solid state. Notably, the π–π interactions of CN-PDI in chloroform are even stronger than in the solid state.

3.3. Electrochemistry of compounds CN-NDI and CN-PDI

CV is a valuable tool to study reversible redox behavior, electrochemical stability and to get information about HOMO and LUMO energy values. Cyclic voltammograms of both compounds are shown in Fig. 10. The LUMO energy values were calculated based on the value of 4.8 eV for Fc with respect to zero vacuum level [17,18]. The obtained potentials and the calculated LUMO values are summarized in Table 3.

CN-NDI exhibits two reversible (−0.89 and −1.34 V) reduction steps in solution. The corresponding cathodic and anodic peak separation value for each reversible reduction

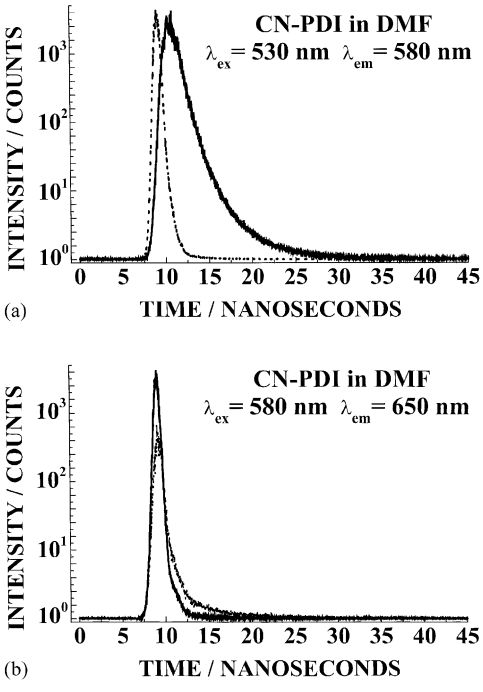

Fig. 7. Fluorescence decay curves of 10^{-5} M CN-PDI, $\lambda_{exc} = 530$ nm and $\lambda_{em} = 580$ nm (a) and CN-PDI, $\lambda_{exc} = 580$ nm and $\lambda_{em} = 650$ nm (b) in DMF.

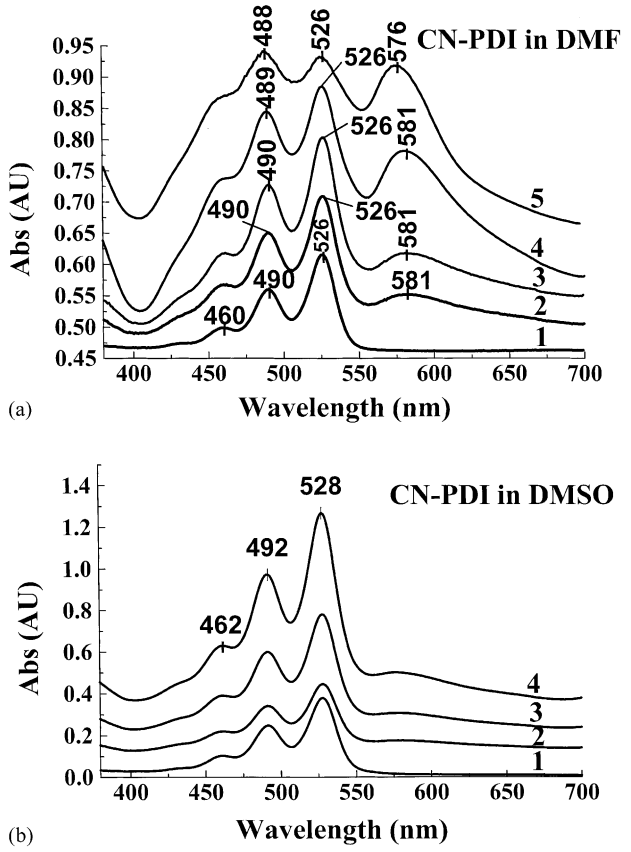

Fig. 8. Effect of concentration on the electronic absorption spectra of CN-PDI in DMF (a) 5: 2×10^{-4} M, 4: 1×10^{-4} M, 3: 5×10^{-5} M, 2: 2.5×10^{-5} M, 1: filtered solution through a 0.2 μm SPR microfilter and DMSO (b) 4: 1×10^{-4} M, 3: 5×10^{-5} M, 2: 2.5×10^{-5} M, 1: filtered solution through a 0.2 μm SPR microfilter.

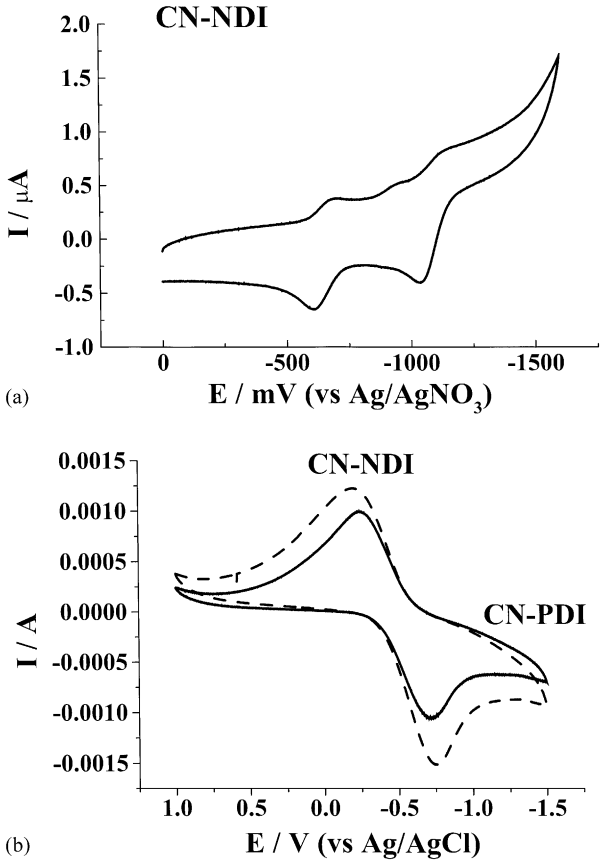

Fig. 10. Cyclic voltammograms of CN-NDI (a) in chloroform/supporting electrolyte: TBAPF6, scan rate: 100 mV s^{-1} and solid state cyclic voltammograms of CN-NDI and CN-PDI (b), supporting electrolyte: $NaClO_4$, scan rate: 100 mV s^{-1} at 25 °C.

step is approximately 60 mV at a scan rate of 100 mV s^{-1} as expected for a fast reversible single electron transfer.

CN-PDI has good solubility in DMF and DMSO. Unfortunately, these solvents are not useful for voltammetry measurements for these compounds because these solvents are reduced in the same range. Solid state voltammograms of the two compounds have identical reduction potentials ($E_{1/2} = 0.48$ V vs. Ag/AgCl). The LUMO energies are calculated as 3.96 eV for CN-NDI and CN-PDI, which is very close to the LUMO energy of CN-NDI in solution.

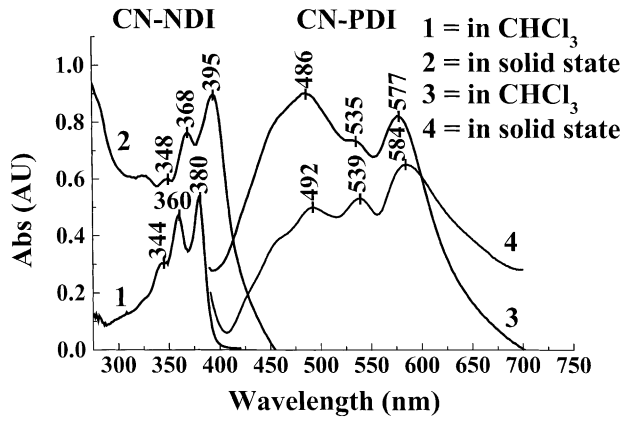

Fig. 9. Electronic absorption spectra of CN-NDI and CN-PDI in the solid state and in $CHCl_3$ solution.

3.4. Thermal stability

CN-NDI and CN-PDI exhibit no glass transition temperatures in the DSC runs (first and second heating) up to 300 °C (CN-NDI) and 350 °C (CN-PDI) (Fig. 11). Thermogravimetric analysis of CN-NDI shows higher thermal

Table 3
CV data of CN-NDI and CN-PDI

	E_{Red} vs. Fc (V)	LUMO (eV)
In solution		
CN-NDI (in $CHCl_3$)	−0.89	−3.91
	−1.34	
In solid state		
CN-NDI	−0.84	−3.96
CN-PDI	−0.84	−3.96

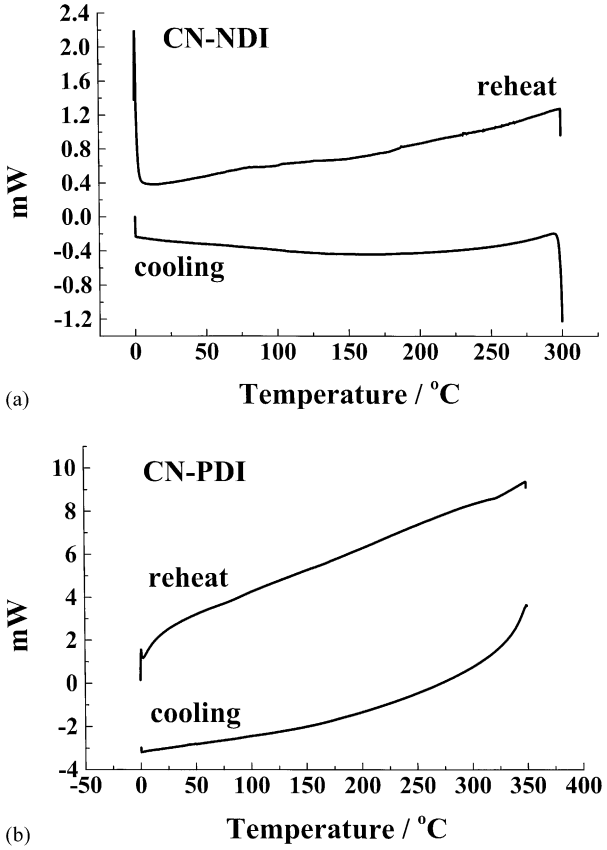

Fig. 11. DSC thermograms of CN-NDI (a) and CN-PDI (b).

stability comparing to Phenyl-NDI. CN-NDI does not loose weight up to 477 °C (Fig. 12) meanwhile Phenyl-NDI starts to loose weight about 437 °C (Fig. 12). Similar relationship is observed between CN-PDI and Phenyl-PDI. Whereas the thermogravimetric analysis curve of CN-PDI shows no weight loss up to 565 °C, Phenyl-PDI starts to loose weight at 543 °C (Fig. 12). Obviously, the cyano (CN) group supports the additional thermal stability.

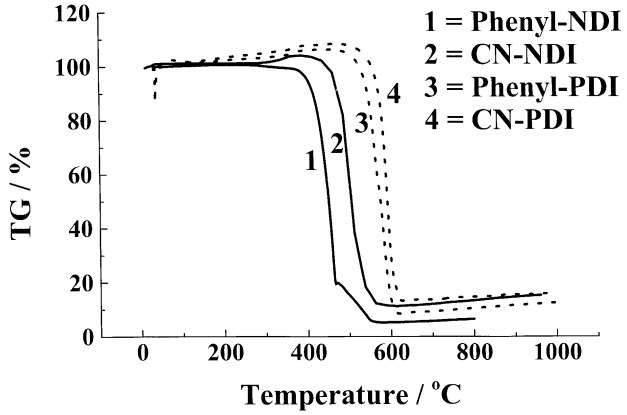

Fig. 12. Thermogravimetric analysis curves of Phenyl-NDI (1), CN-NDI (2), Phenyl-PDI (3) and CN-PDI (4) at a heating rate of 5 K/min in oxygen.

4. Conclusion

The synthesis of CN-NDI and CN-PDI could not be achieved with the common way, which is described in the literature [10,11]. The electron accepting cyano group in the amine presumably prevents the imidization. We have achieved the synthesis of CN-NDI and CN-PDI under special conditions in high yield.

The compounds have poor solubility in non-polar organic solvents, in addition to good photochemical and thermal stability. TGA measurements demonstrated that the existence of CN group on both of the compounds caused to increase thermal stability at least 100 °C.

CN-NDI has a quite narrow spectral range (300–400 nm) comparing to CN-PDI (400–700 nm). PDI dye aggregates even at 10^{-5} M concentration whereas the spectral data of unaggregated form is very similar to that of solutions. Drastic changes in the UV absorption spectrum, i.e. wavelength range and peak positions of solutions vs. solid state, are attributable to the strong intermolecular interaction in the solid state.

Both compounds have low fluorescence quantum yields. They undergo reversible electron oxidation and reduction. Calculated LUMO values for CN-NDI and CN-PDI are identical in the solid state. Also, the LUMO energies of the compounds in the solid state are very close to the LUMO energy of CN-NDI in solution. The CN-PDI is weakly fluorescent with a lifetime of 3.8 ns ($\lambda_{exc} = 530$ nm and $\lambda_{em} = 580$ nm). The additionally observed longer lifetime of 4.6 ns is ascribed to emission from the dye aggregates ($\lambda_{exc} = 580$ nm and $\lambda_{em} = 650$ nm).

Both compounds, CN-NDI and CN-PDI, are promising as electron acceptors for singlet-state electron transfer reactions. Further, CN-PDI could in our opinion be a promising candidate for application in organic solar cells because of its wide spectral absorption range, the excellent photochemical stability together with reversible electron exchange capacity and its tendency towards facile and even spontaneous aggregation.

Acknowledgements

This work was supported by the Scientific Research Council of Turkey (TUBITAK, TBAG-1707). We would like to acknowledge and thank Prof. Fritz Scholz for help with the solid state voltammetry.

References

[1] P. Pösch, M. Thelakkat, H.W. Schmidt, Syn. Met. 102 (1999) 1110.
[2] B.A. Gregg, Chem. Phys. Lett. 258 (1996) 376.
[3] Rudiono, F. Kaneko, M. Takeuchi, Appl. Surf. Sci. 142 (1999) 598.
[4] H. Tian, P. Liu, W. Zhu, E. Gao, D. Wu, S. Cai, J. Mater. Chem. 10 (2000) 2708.
[5] T.C. Barros, S. Brochsztain, V.G. Toscano, F.B. Filho, M.J. Politi, J. Photochem. Photobiol. A 111 (1997) 97.

[6] D. Meissner, J. Rostalski, Syn. Met. 121 (2001) 1551.
[7] Y. Zhao, M.R. Wasielewski, Tetrahedron Lett. 40 (1999) 7047.
[8] J. Rotalski, D. Meissner, Solar Energy Mater. Solar Cells 63 (2000) 37.
[9] K. Petritsch, J.J. Dittmer, E.A. Marseglia, R.H. Friend, A. Lux, G.G. Rozenberg, S.C. Moratti, A.B. Holmes, Solar Energy Mater. Solar Cells 61 (2000) 63.
[10] H. Langhals, Heterocycles 40 (1) (1995) 477.
[11] H. Icil, D. Uzun, E. Arslan, Spectrosc. Lett. 34 (3) (2001) 605.
[12] F. Scholz, B. Meyer, in: A.J. Bard, I. Rubinstein (Eds.), Electroanalytical Chemistry. A Series of Advances, vol. 20, Marcel Dekker, New York, 1998, pp. 1–82.
[13] F. Würthner, C. Thalacker, S. Diele, C. Tshierske, Chem. Eur. J. 7 (2001) 2245.
[14] N.J. Turro, Molecular Photochemistry, Benjamin, London, 1965, pp. 44–64.
[15] J. Karolin, L.B.A. Johansson, U. Ring, H. Langhals, Spectrochim. Acta, Part A 52 (1996) 747.
[16] S. Green, M.A. Fox, J. Phys. Chem. 99 (1995) 14752.
[17] H.M. Koepp, H. Wendt, H. Strehlow, Z. Electrochem. 64 (1960) 483.
[18] J.L. Bredas, R. Silbey, D.S. Bourdreaux, R.R. Chance, J. Am. Chem. Soc. 105 (1983) 6555.